*The 2014 World Congress on*
***Advances in Civil, Environmental, and Materials Research (ACEM14)***
*Busan, Korea, August 24-28, 2014*

# Field measurements and CFD simulation for wind effect on PV solar panels mounted on flat roofs

*Ya Liu[1)] Elena Dragomirescu[2)]

[1), 2)] *Department of Civil Engineering, University of Ottawa, Ottawa K1N 6N5, Canada*
[1)] elndrag@uottawa.ca

## ABSTRACT

Wind-induced loads on photovoltaic (PV) solar panels installed on roof tops, are of main concern when designing the system; a detailed comparison between the guidelines and design codes ASCE7-05 (2005) and SEAOC (2013) and field measurements were conducted for a PV solar panel installed on the Mann Parking Building of the University of Ottawa. The PV panel was instrumented with a total of 26 strain gauges, on both surfaces of the panel and data was collected for 5 months. It was noticed that the roof wind zone, building edge and the parapet were the main elements affecting the estimated wind load value on each PV panel. The maximum wind load of 1,208 N was obtained on the northwest corner of the PV solar panel arrays, and the minimum wind load of 806 N was determined for the center of PV solar panel arrays. The field measurements indicated that the highest wind - induced stresses are on the lower edge of the PV panel and the lowest stresses are on the middle point of the front surface of the PV solar panel; however, for the back surface of the PV panel the opposite situation was noticed, the highest stresses are in the middle of the panel, and the lowest stresses are on the lower edge of the back surface of the PV solar panel. In general, for the front surface, the sensors which are on the edge of PV solar panel are subjected to higher stresses than the sensors on the center of PV solar panel, while the sensors on edge of the back surface are sheltered by the frame so that the stresses acting on them are lower than the for the center lines. The same results were confirmed through a CFD simulation performed for 10 m/s and 26 m/s wind speed for 0° and 180° angles of attack, employing the LES algorithm.

## 1. INTRODUCTION

The most common devices of collecting the solar energy are the photovoltaic (PV) solar panels, which are usually installed on flat or inclined building roofs, or at terrestrial level. Due to their exposure to high altitudes and therefore high wind speeds, several

[1)] Graduate Student
[2)] Professor

damages of PV solar panels and solar water heating systems installed on flat-roofs have been reported by Chung et al, (2007) for Taiwan region, where an average of 3.5 typhoons are recorded each year. Due to such wind-induced hazards, a thorough experimental verification was conducted by numerous researchers. Aly (2013) studied the effects of model scale for the ground-mounted solar panels, wind tunnel experiments and by the use of CFD simulations and concluded that under certain conditions, the results from CFD simulations could become more accurate than the results obtained from the wind tunnel test. Numerical CFD simulations have also been performed for small groups of PV solar panels by Hangan et al, (2008) and recommendations have been formulated regarding the angle of attack and the critical spacing between the arrays of the PV panels. Bitsuamlak et al, (2010) compared the results from numerical LES (Large Eddy Simulation) analysis with wind tunnel tests for ground mounted stand-alone and arrays of PV solar panels and they found very small differences between the pressure coefficient distribution on the middle and on the side panel of each row. Radu et al (1986) performed a wind tunnel experiment on the steady wind pressures on solar collectors mounted on flat-roofed medium-rise buildings. Their study was carried out in an open jet boundary-layer wind tunnel for a scaled model of a five-story rigid building of apartments supporting a roof with solar collectors mounted in simple and consecutive rows. Chung, et al (2010) carried out an experimental study in a low-speed wind tunnel, to investigate the mean surface pressure distributions and uplift force at different wind speeds, on solar collectors mounted on flat roofs of low rise buildings situated in typhoon prone regions. Also wind tunnel tests have been performed for singular PV panels (Hangan et al, 2008) on three parallel arrays of PV panels (Shademan et al., 2009) and pressure distribution, drag and lift coefficients, overturning of middle panels and sheltering effect caused by the primary row of panels were investigated. Field measurements on PV solar panels are very difficult to obtain especially for the upper surface of the panels, because during their operation, obstructing equipment cannot be installed on the upper surface bearing the silicon cells, because this might interfere with the collection of solar energy. Hence most of the field measurements are performed for the back surface of the PV panels, or on the supporting frame, and by the aid of the formulations recommended by the designing codes, the wind force on the upper surface of the panel is determined. Based on such measurements, the Structural Engineers Association of California's (SEAOC) Solar Photovoltaic System Committee a report was developed which focuses the characteristics of wind flow on solar photovoltaic panels arrays installed on flat roofs of low-rise buildings. The estimation of wind loads determined from the measurements were verified with the values obtained based on the gust factor and wind pressure coefficient (GCn) as per the methodology recommended by the ASCE7-05 and the SEAOC report (2013). The wind-structure interaction is actually much more complex, and the strain measurements on the PV solar panel will not capture the actual cause of the deformation of the PV panel, this being directly related to the wind flow patterns formed around the PV panel and its frame support system. In order to verify the wind flow patterns and the pressure distribution at various points on the surface of the PV panel, Computational Fluid dynamics (CFD) simulations were performed by the aid of the Ansys Fluent Software. Wind speeds of 10 m/s and 26 m/s, for angles of attack of $\alpha$ = 0° and 180°.

## 2. EXPERIMENTAL SETUP AND THE PV SOLAR PANEL CONFIGURATION

The features of 180 watt maximum power poly-crystalline PV solar panel (Figure 1) are high conversion efficiency based on leading innovative photovoltaic technologies, and if properly installed it can withstand high wind-pressure, snow loads, and extreme temperature variations. The geometrical dimensions of one PV solar panel are 1.580 m × 0.808 m × 0.035 m (H×W×D). The PV solar panel is installed on a 2.10 m×0.83m ×1.40 m (H×W×L) frame which ensures a tilt angle of up to 35° (Fig. 1).

Fig. 1 Site location of PV solar panel: a) Supporting frame, b) Front surface sensors layout, c) Back surface sensors layout

The instrumentation used was composed of a total of 26 strain gauges, a AM16/32B multiplexer and a CR 1000 datalogger. An anemometer and an external thermometer were also available at the site for collecting weather data. The PV solar panel is installed on the flat roof of Mann Parking Building of the University of Ottawa. Most of the experiments presented in literature have replaced the PV solar panels with plywood, or plastic panels and they placed the sensors on the centre vertical and horizontal lines of the models, on both faces. The current research is using the strain gauge sensors on the front surface of a real PV solar panel, on the limited space existing between the solar cells. A total of 13 strain gauges were placed on the centre cross lines on both faces of the panel, as schematically represented in Fig. 2. For some locations close to the centre of the panel, bi-axial sensors were used (sensors numbers 5,6 7,8 and 9,10 in Fig. 2).

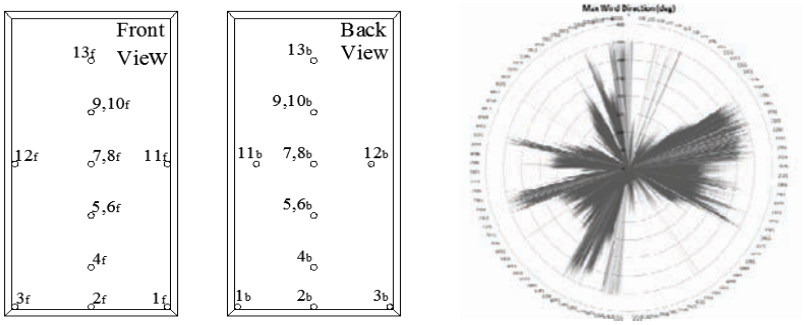


Fig. 2 a) Strain gauges sensors location b) Wind speed direction for the Jan 2014

Wind data was collected for the direction of the wind speed (Figure 2 b) and for the intensity of the wind speed Figure 3, only the maximum values being reported here. Two dominant wind directions were recorded, between 340° and 350° and the second one between 190° and 220°. The PV solar panel orientation installed on the flat roof was set as north-south, where north is considered as 0° and south is 180°.
The wind speed intensity for the Nov 2013 - Mar 2014 period varied between the highest values of 10 - 12 m/s.

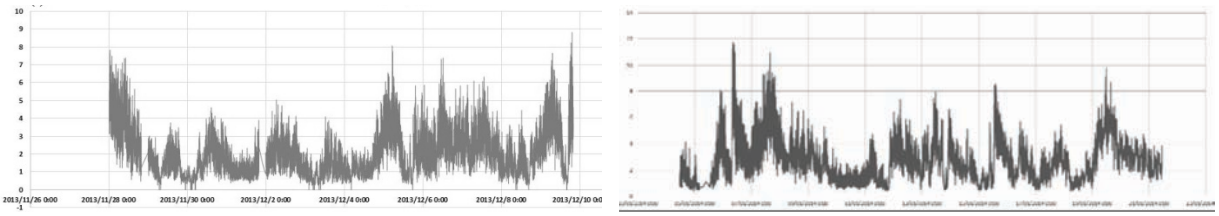

Figure 3. Maximum wind speed for the Dec 2013 and Jan 2014

Figure 4 shows the stress variation for the sensors located on the lower margin (sensors 1 and 2) and on the middle horizontal line (sensors 7 and 11) of the front surface of the PV solar panel. Sensor 1, located at the lower corner of the PV panel, recorded the highest maximum stress and minimum stress, hence the highest stress variation; rather, sensor 7, at the middle of the PV panel has the lowest maximum stress and minimum stress. Also was noticed that the stresses recorded by sensor 11 are slightly higher than the ones from sensor 7, both located on the middle horizontal line of the PV panel. Figure 5 shows the stress distribution on back surface of the PV solar panel; the stress magnitude is similar with the one recorded for the front surface, however, the variation is opposite (mirrored) for each corresponding sensor and wherever the stress is increasing on the front surface, it would decrees on the back surface. Hence sensor 7 in the middle of the PV back panel has the highest values for maximum and minimum stresses; rather, sensor 2, on the horizontal line, near the lower edge of the panel, has the lowest maximum and minimum stresses. The stresses recorded by sensor 11 are lower than the stresses from sensor 1, located on the lower edge of the panel, in the corner of the panel.

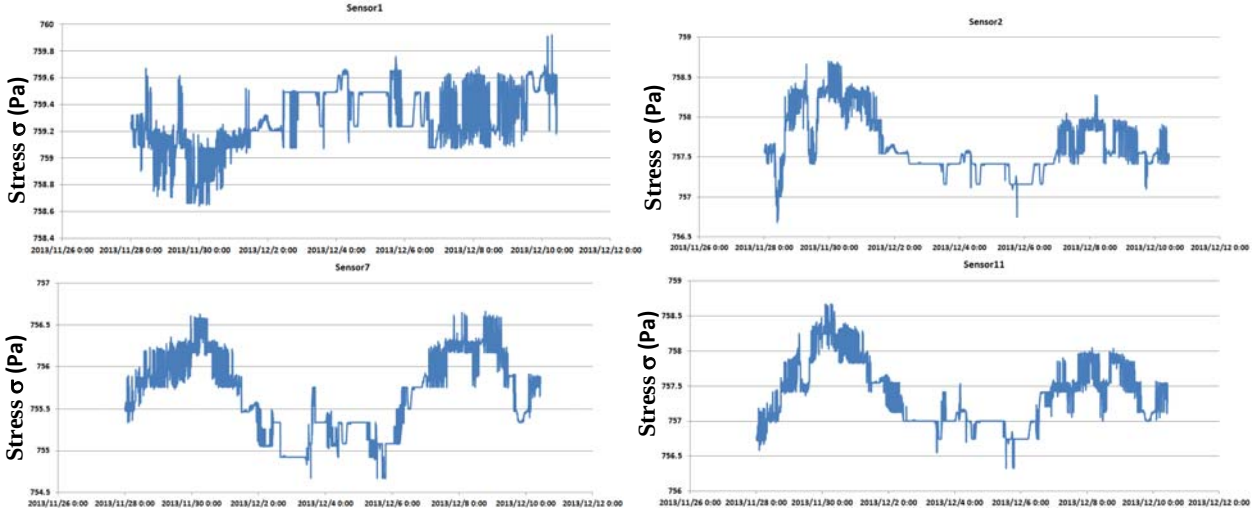


Figure 4. Stress data at selected locations on the front surface of the PV panel

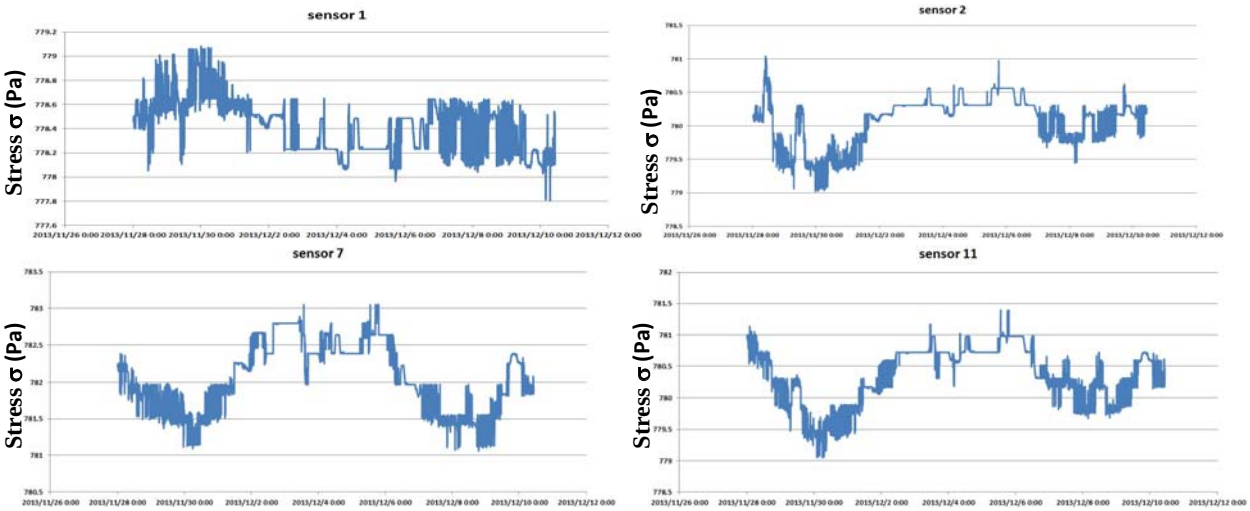


Figure 5. Stress data at selected locations on the back surface of the PV panel

In order to investigate the distribution of force on both sides, the panel was divided in 18 equal patches on which the sensors were placed considered as the sensor(s) as tributary area. Finally the average force on the front surface of PV solar panel 967.207 N and the average force on the back surface of PV solar panel was 996.465 N.

## 3. DESIGN CODES FOR PV SOLAR PANELS

The current project focused on instrumenting and measuring the wind-induced pressures and forces for a singular PV solar panel, results which will be used for calibrating larger models and bigger cluster arrangements of PV solar panels. The SEAOC (2013) design specifications provides the calculation procedure for PV panels contained in one of the layers located in three different roof zones: interior zone, edge zone, and corner zone. If solar panels are mounted on the roof, the corner zones have much higher wind induced pressure than on the roof itself. As the height above the roof or length of the module increases, the wind loads increase. For most of the solar photovoltaic installations, the maximum height above the roof surface (h2) should be limited to 4 feet and the length (lp) should be limited to 6 feet 8 inches; the gap between the modules and the roof surface (h1) should not exceed 2 feet to prevent creation of excessive uplift. A reduction factor, γc (0.8~1.0), is recommended for reducing the wind loads for shorter modules, which applies only to the higher tilt angle ($\omega$ = 15° to 35°). If there are parapets on the roof, it worsens the wind loads on solar modules, so that the codes limit the parapet height to 4 feet unless the GCn values are increased by a 1.3 factor. For considering low-rise buildings, ASCE7-05 reports standardized graphs representing the wind pressure coefficients GCn as function of the normalized wind area which is different than the effective wind area. 15 feet is set as a lower limit on the height of building. Two GCn curves are created one for lower tilt angle modules in the range of 1° to 5° and one for higher tilt angle modules in the range of 15° to 35°. The calculation of the wind induced forces was performed considering several scenarios of a single PV panel placed in the corner of the roof and in the centre

of the PV panels' array (location 1), in the same corner of the roof and in the corner of the PV panels' array (location 2) and on the edge of the roof and in the corner of the PV panels' array (location 3). To convert the allowable stress design wind loads to the ASCE7-05 Design Code, multiplying the estimated wind loads by a safety factor of 0.6 was considered. The average load distributed along the panel would be transferred to the fasteners connecting the panel to the frame. The pressure coefficient for each roof zone were read from the tables provided in ASCE7-05, based on effective wind area A = 3.23 feet$^2$ and normalized wind speed area An = 8.0 and are represented in Table 1.

Table 1. Pressure coefficient GCn

| Roof Zone | 0°~15° | 15°~35° | (15°~35°)* γc |
|---|---|---|---|
| Edge | 1.48 | 2.15 | 1.95 |
| Corner | 1.70 | 2.60 | 2.36 |

Where the chord length adjustment factor (γc) for the GCn at higher tilt angles of 15°≤ω≤35° is obtained by interpolating γc = 0.6+0.06 × lp =0.6+0.06 × 5.18ft$^2$.
The edge factor (E) was determined considering the characteristic height, $h_c$ = min($h_1$,1ft) + $l_p$sinω, where $h_c$ was 3.09 feet, except when evaluating a panel towards a building edge unobstructed by panels, then $h_c$ = 0.1$a_{pv}$. Also $h_c$ was 2.0 feet when evaluating E for a building roof with PV panels unobstructed by the edge. The parapet height factor ($\gamma_p$) was considered $\gamma_p$ =1.0, since $h_{pt}$ < 4.0 feet. The calculation of $GC_n$ varied between 1.95 and 2.36, for different locations of the PV panel inside the array and for the corresponding roof regions
To complete the calculation of the maximum wind load on each PV module fastener to the supporting racking system, the wind velocity pressure ($q_h$) must be determined based on the ASCE 7-05, Equation 29.3-1, considering the exposure coefficient at 20 feet was $K_z$ = 0.9, $K_{zt}$ = 1.0 and $K_d$ = 0.85 (ASCE 7-05, Table 26.6-1). For a wind speed corresponding to Ottawa region of V = 110 mph, a velocity pressure of $q_h$ =23.70 lbs/ft$^2$ was determined.
As per the calculation of the final forces, was noticed that the corner location of the roof (location 2) has the maximum net pressure coefficient, and LRFD pressure value and the maximum wind load 1,208 N is acting on it. The panel situated at location 1 registered a force of 806 N and the panel situated in the roof edge zone (location 3) had 998 N

## 3. CFD NUMERICAL SIMULATION FOR PV SOLAR PANEL

A simulation domain of 20 m by 30 m was created using a coarse mesh of 2.55 mil cells (Fig.6 a) while around the PV panel model of dimensions 2m × 1m, a circular region of much thinner mesh was simulated with 1.5 mil cells, allowing for more accurate computation in this area (Fig. 6 b). Initially smooth flow was simulated until convergence was achieved thereafter the LES algorithm which determines the fine eddy formations from the large eddies through the filter width of the subgrid scale, which was chosen here as the width of the element of the mesh.

A time step of 0.0003s was set, and the number of simulations was limited to 1000. The no slip no penetration boundary conditions were applied to the PV panel and its mounting frame. The side walls though were set as symmetry conditions, so that flow can pass through their boundaries without bouncing back hence without affecting the precision of the flow formation on the PV panels. The geometry used for the CFD simulation does not have the exact same configuration and dimensions as the PV panel monitored on the Mann Building roof, because the installation of this panel was completed after the CFD simulation was performed. Incoming velocities of 20 m/s and 26 m/s were used which correspond to Re of $1.5\times10^6$ and $2.0\times10^6$, the chord of the panel being used for this estimation. Pressure distribution along the upper and lower surfaces for the panel were extracted, velocity profiles at the middle of each panel, average force coefficients for middle panels and finally three-dimensional visualization of the swirl turbulent formations were monitored.

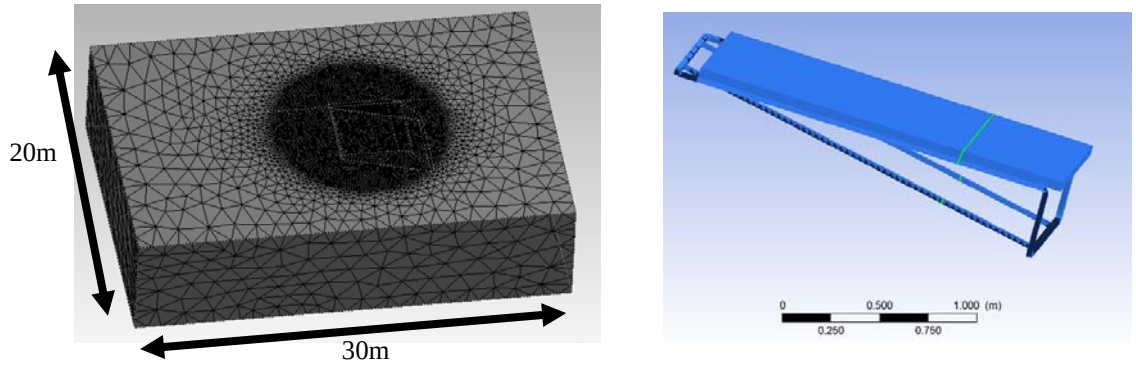


Fig. 6 Mesh details for (a) Mesh domain (b) A singular PV panel

The measurements have shown that the dominant wind speed directions were between 340° and 350° and between 190° and 220°, therefore in the CFD simulation the most critical cases of 0° and 180° angles of attack were chosen and results for slightly higher wind speed of 26 m/s were presented herewith.

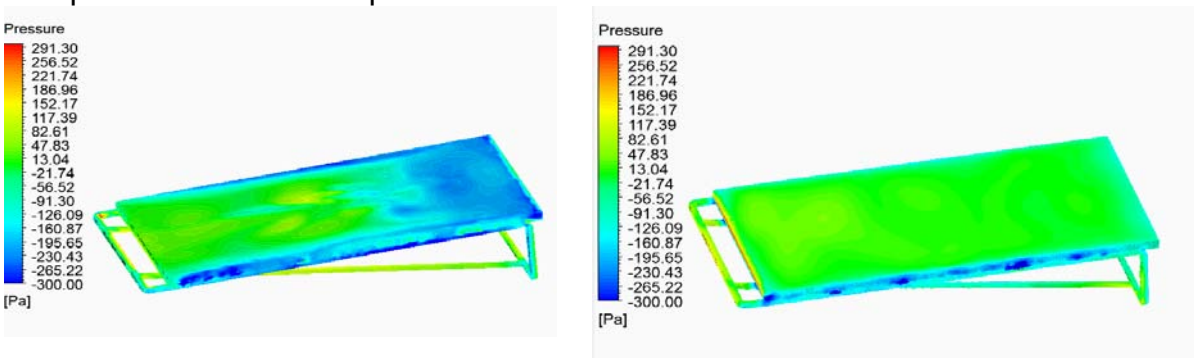


Fig. 7 Surface pressure for the PV panel for 26 m/s (a) $\alpha$ = 0° and (b) $\alpha$ = 180°

The pressure distribution determined for $\alpha$ = 0°, when the incoming flow approaches the panel from the upper edge, showed a high suction of up to -300 Pa at the upstream edge of the PV panel, but a positive pressure, around the middle region of the panel (Fig. 7a). For $\alpha$ = 180°, when the incoming flow approaches the PV panel from its lower

edge, the pressure distribution on the surface of the PV panel was almost invariable on the upper surface of the panel, however on the edge of the panel pressure fluctuation was signalled (Fig. 7b). Wind-induce pressure in a transversal plane taken at the middle of the PV panel and another longitudinal plane sectioning the entire length of the panel were reported and a high suction was confirmed around the edges of the panel, on both sides, and vortex-like structures formed towards the middle of the upper surface (Fig. 8 a). For the longitudinal plane the detachment of the incoming flow near the upper edge of the PV panel could be noticed through the high suction of up to -300 Pa at the top of the PV panel.

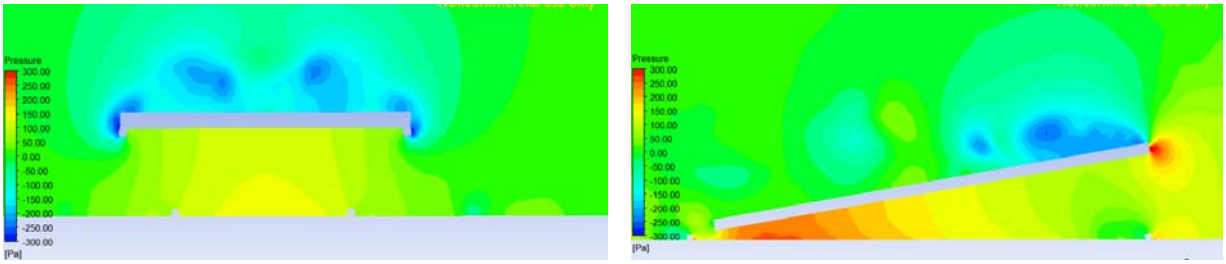


Figure 8 Pressure distribution for 0° and 26 m/s a) Upper edge of the PV solar panel b) Middle vertical plane of the PV solar panel

A three-dimensional visualization of the swirl formations determined by Q-criterion velocity method, showed that for the 0° the re-attachment of the flow incoming from the top edge will expose the middle part of the panel to turbulent flows (Fig. 9 a), which explains the variation of negative pressure in Fig.7 a; also, along the edges of the panel two longitudinal vortices were formed which induced the suction on the panel's edges indicated by the blue color in Fig. 7 a. Several turbulent formations can be noticed in Fig. 9 a, on top of the PV panel, which are associated with the negative pressure vortices visualized in Fig. 8 a. Turbulence is absent on the upper surface of the PV panel for 180° (Fig. 9 b), which is in conformity with the uniform pressure distribution shown in Fig. 7 b. The swirls determined a turbulent flow shedding downstream the panel, from the top edge (Fig. 9 b) and the lateral edges of the PV panel were enveloped by slim longitudinal vortices formed on both sides hence negative pressure is expected.

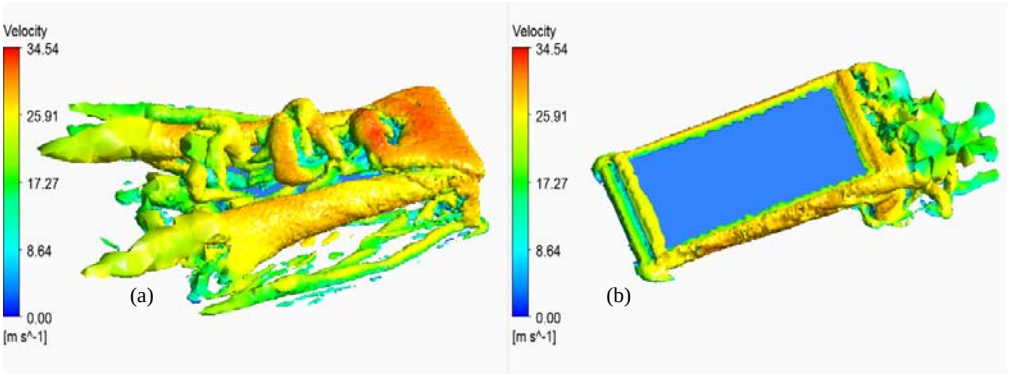


Figure 9. Three-dimensional visualization of turbulent swirl formations for (a) $\alpha$ = 0°, upper surface, (b) $\alpha$ = 180°, upper surface

## CONCLUSION

Smooth flow effect was investigated for a 2 m by 1 m PV solar panel through the use of CFD, LES simulations. Angles of attack of 0° and 180° were considered and wind speeds of 10 m/s and 26 m/s. From the pressure data it was noted that the center region of the PV panel is exposed to turbulent flow formations and that suction dominated on its upper edge, with a suction of up to -300Pa. Hence, a uniformly distributed force on the surface of the PV panel of approximately up to 600 N can be estimated, which is much lower than the maximum design forces detailed below, thus proving that the PV panels is within the safe margins. Based on the calculation procedure recommended by the SEAOC and ASCE7-05 design codes, the maximum wind load on the PV solar panels mounted on the roof tops is obtained for different locations considering the roof wind zone and location of the PV panel inside the array. The net pressure coefficient GCn was estimated (ASCE7-05) and a conversion to LRFD force estimation was considered and was noticed that for panels at the corner location of the roof (location 2) the maximum design wind load was 1,208 N while for the panels situated at location 1 a design force of 806 N was determined. For the panel situated in the roof edge zone (location 3) a 998 N force was calculated.
From the field measurements performed on the PV solar panel installed on the roof of Mann parking, the highest stresses are on sensors 1 and 3 on the lower edge of the PV panel and the lowest stresses are on sensor 7 on middle point of the front surface of the PV solar panel, however, for the back surface of the PV panel the opposite situation was noticed, the highest stresses are in the middle of the panel, on sensor 7 and the lowest stresses are on sensor 1 on the lower edge of the back surface of the PV solar panel. On the front surface, the sensors which are on the edge of PV solar panel are subjected to higher stresses than the sensors on the centre of PV solar panel; rather, the sensors on edge of the back surface are sheltered by the frame so that the stresses acting on them are lower than the sensor which are on the centre lines.
The average forces determined from the experiments performed on the PV solar panel are very close to the average force on the location 3 in the code study; however, they are not in the same roof zone. The experimental PV panel and the code location 2 have the same position on the roof. Both of them are in the corner of roof and next to the parapets, and the average force on location 2 is 1,208 N which is slightly higher than the experimental one. It shows that the zone of the roof and the parapets influence the estimation of the wind load on the PV solar panel.

## REFERENCES

Aly M. Aly, Bitsuamlak. G, (2013), “Aerodynamics of ground-mounted solar panels: Test model scale effects”, *in Proc. of The 13th American Wind Eng. Conf.*, Seattle, USA
ASCE 7-05, (2005), Chapter C6: Wind loads.
Bitsuamlak, G.T., Dagnew, A.K., and Erwin, J., (2010), “Evaluation of wind loads on solar panel modules using CFD”, *in Proc. of The Fifth International Symposium on Computational Wind Engineering*, Chapel Hill, North Carolina, USA May 23-27.
California Structural Engineers Association, (2013), “Wind Design for Low-profile Solar Photovoltaic Arrays on Flat Roofs”.

Chung, K., Chang, K., Liu, Y., (2008), “Reduction of wind uplift of a solar collector model”. *J. Wind Eng. Ind. Aerodyn.,* **96**: 1294-1306.
Chung, K., Chang K., Chou, C., (2011), “Wind loads on residential and large scale solar collector models”. *J. Wind Eng. Ind. Aerodyn.,* **99(1)**: 59-64.
Hangan, H., (2010), “A study of wind effects for solar power products panel mount system”, *Report BLWT-SS8-2010*, Alan G. Davenport Wind Engineering Group.
Pratt, R. N. and Kopp G., (2013), “Velocity measurements around low-profile tilted, solar arrays mounted on large flat-roofs, for wall normal wind directions”, *J. Wind Eng. Ind. Aerodyn.,* **123 (A)**: 226-238.
Radu, A. Axinte, E. and Theohari, C., (1986), “Steady wind pressures on solar collectors on flat-roofed buildings”, *J. Wind Eng. Ind. Aerodyn.,* **23**: 249-258.
SEAOC, 2013, Solar Photovoltaic Systems, Wind design for low-profile solar photovoltaic arrays on flat roofs.
Schellenberg, A., Maffei, J., and Tell, K., (2013), “Structural analysis and application of wind loads to solar arrays”. *J. Wind Eng. Ind. Aerodyn.* **123 (A)**: 261-272.
Shademan, M., Hangan, H., (2009), “Wind Loading on Solar Panels at Different Inclination Angles”, in Proc. of *11th Americas Conference on Wind Engineering*, San Juan, Puerto Rico.
Shademan, M,. and Hangan, H., (2010), “Wind loading on solar panels at different azimuthal and inclination angles”, in Proc. of *The Fifth International Symposium on Computational Wind Engineering*, Chapel Hill, North Carolina, USA May 23-27.